WAVE SLOSHING INSIDE A RESERVOIR

Tiago Konno de Dornellas Cysneiros, tkdornellas@gmail.com
Roger Matsumoto Moreira, roger@vm.uff.br
Raphael David Aquilino Bacchi, raphael@esss.com.br
Laboratório de Dinâmica dos Fluidos Computacional, Universidade Federal Fluminense, R. Passos da Pátria 156, bl.D, sl.563A, Niterói, RJ, CEP: 24210-240.

Abstract. The present work aims to model numerically the generation and propagation of waves in a reservoir, represented by a impermeable box, with a flat horizontal bottom and four vertical walls. A horizontal or vertical harmonic motion is imposed at the container, which is partially filled with water, with the free surface's initial condition being at still water condition. The boundary value problem is solved by means of the commercial code ANSYS CFX 11.0 with its homogeneous free surface model. Results are compared with experiments done by Bredmose et al. (2003). Interesting features at the free surface are obtained and discussed.

Keywords: wave sloshing, free surface flow, computational fluid dynamics.

1. INTRODUCTION

An imposed movement on a partially filled reservoir can generate free surface waves. Large accelerations can cause violent wave impacts at its walls, as in fuel tanks in trucks, aircraft, spacecraft or ships. Those impacts induce hydrodynamical forces which may cause the container's rupture, instability and/or loss of maneuverability of such vehicles. The sloshing phenomena represent a classical eigenvalue problem, having been studied by illustrious scientists like Poisson, Rayleigh, Kirchhoff and Lamb.

Ockendon & Ockendon (1973) find the resonant wave frequencies for a 2D box of length πL and depth hL to be:

$$\omega = [g \, n \, tanh \, (nh)/L]^{1/2} \tag{1}$$

where g is the acceleration of gravity and n is the wave number. Resonance occurs when the fluid is forced to oscillate at these frequencies. In a more recent study, Mendes & Moreira (2006) e Mendes (2007) found numerically the formation of such resonant surface waves by means of a fully nonlinear boundary integral solver.

The generation of patterns of steep, standing waves is an important feature observed in sloshing motions. Bredmose *et al.* (2003) noted that two distinct types of behavior may coexist in a confined tank: a violent, brief impact of the liquid on the container wall and long, lasting, large amplitude sloshing motions. If certain driving frequencies are imposed, vertical accelerations in a container may induce the growth of standing waves. Bredmose *et al.* (2003) report numerically and experimentally the formation of "table-top" breaking waves, also known as Faraday waves. In another nonlinear phenomenon, Longuet-Higgins (2001) shows that vertical jets can also result from high amplitude standing waves, which is known as the "bazooka" effect. The free surface flows mentioned above have gravity as its main restoring mechanism. On a smaller scale, however, surface tension may affect significantly wave properties. Small scale ripples, or capillary waves, occur due to external accelerations imposed on the reservoir. Billingham (2001) finds that, under zero gravity conditions, periodic and chaotic solutions and solutions where the topology of the fluid changes, either through self-intersection or pinch off, are possible.

In Brazil, the exploration of oil and gas occurs mostly offshore, with Campos basin being responsible for approximately 70% of the national production. Over the recent years, the floating production systems - semi-submersible platforms and FPSOs - have had their storage tanks increased constantly in response to a growing demand for oil.

In that context, it is of paramount importance to understand the mechanics behind those waves, uncovering the main driving modes that could provoke violent impacts on the reservoir structures, compromising stability and integrity of those ships.

Despite the broad availability of commercial computational fluid dynamics (CFD) software, many of their alleged capabilities in recreating real fluid behavior, sloshing included, remain to be validated against experimental data. The present work aims to compare numerical results obtained using a commercial software package to previous experimental and numerical results from Bredmose *et al.* (2003) - namely experiments H10 and V21.

2. PROBLEM

The behavior of the free surface flow in a moving tank is studied in the present paper. The tank in Bredmose *et al.* (2003) is the same for the two experiments, and its internal dimensions are 1480 x 400 x 750 (length x width x height) mm^3. It is partially filled with water to a level of 155 mm in the horizontal sloshing experiment H10 and 210 mm in the vertical sloshing experiment V21. The input signal for the tank lateral displacement in H10 experiment is

shown in Fig. 1. Notice that the displacement function is composed of three distinct regions. A resonant linear wave frequency for the chosen depth and wave mode is gradually imposed, maintained, and then suddenly removed after t_2. Experiment V21 features horizontal motion followed by vertical motion in order to create standing waves, as can be seen in Fig. 2.
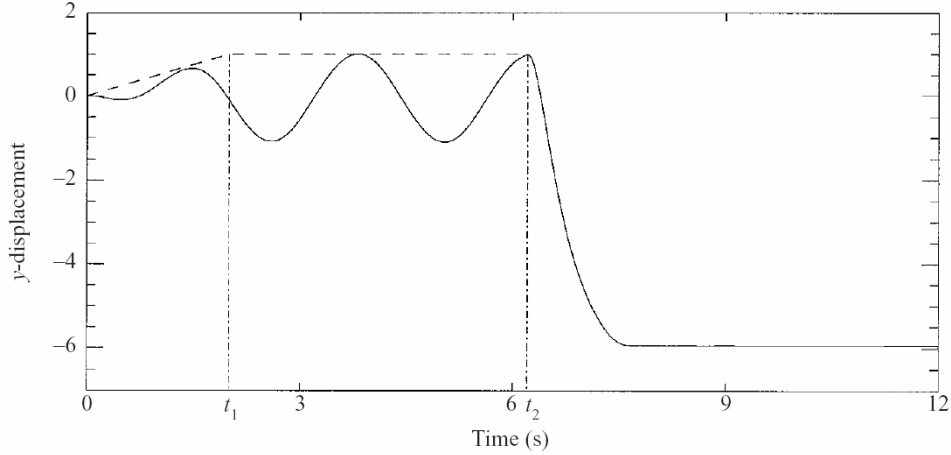

Figure 1. Tank displacement in experiment H10. Displacement scale factor $f=2cm$. (Bredmose *et al.* 2003)
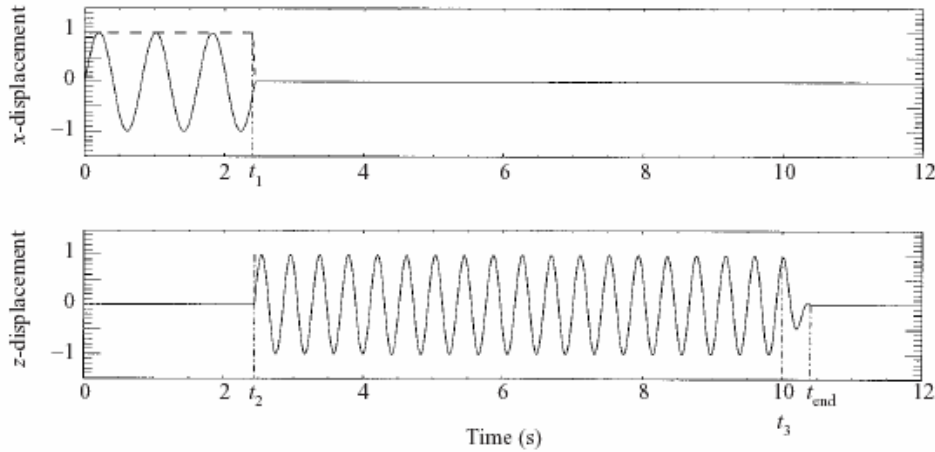

Figure 2. . Tank displacement in experiment V21. (Bredmose *et al.* 2003)

3. ANSYS CFX

ANSYS CFX is a commercial multipurpose CFD code currently developed by ANSYS Inc. The CFX numerical kernel uses the Element Based Finite Volume (EbFV) method to treat generalized unstructured meshes in cartesian coordinates. The discrete system of linearised equations is solved using the Algebraic Multigrid (AMG) method accelerated by the Incomplete Lower Upper (ILU) factorisation technique. The instantaneous equations of mass and momentum can be written as follows in a stationary frame:

$$\frac{\partial \rho}{\partial t} + \nabla \bullet (\rho U) = 0 \tag{2}$$

$$\frac{\partial (\rho U)}{\partial t} + \nabla \bullet (\rho U \otimes U) = -\nabla p + \nabla \bullet \tau + S \tag{3}$$

Where the stress tensor, τ, is related to the strain rate by

$$\tau = \mu\left(\nabla U + (\nabla U)^T - \frac{2}{3}\delta\nabla\bullet U\right) \tag{4}$$

Where μ is the dynamic viscosity, ρ is density of the fluid, p is the static pressure, U is the velocity vector and S is the summation of the source terms. Pressure-Velocity coupling is carried out in a single cell of the collocated grid using a Rhie and Chow like formulation. This solution approach uses a fully implicit discretisation of the equations. In ANSYS CFX, due to the EbFVm, the control volume is generated around each mesh node by connecting all the neighbor element centers and corresponding edge centers by planes, forming a polyhedron. This approach leads to a higher numerical accuracy, because it has many more integration points per control volume (24 for a hexahedral volume and 60 for a tetrahedral volume) than the classical volume method.

3.1. Homogeneous free surface model

The present paper uses the homogeneous free surface model of ANSYS CFX. In homogeneous multiphase flow, a common flow field is shared the two phases (water and air at 25°C and 1 atm), as well as other relevant fields such as temperature and turbulence, i.e.,

$$\phi_\alpha = \phi \qquad 1 \le \alpha \le N_p \tag{5}$$

Where ϕ is transported quantities shared in homogeneous multiphase flow. It is sufficient to solve for the shared fields using bulk transport equations rather than solving individual phasic transport equations as follow

$$\frac{\partial}{\partial t}(\rho\phi) + \nabla\bullet(\rho U\phi - \Gamma\nabla\phi) = S \tag{6}$$

Where:

$$\rho = \sum_{\alpha=1}^{N_p} r_\alpha \rho_\alpha$$

$$U = \frac{1}{\rho}\sum_{\alpha=1}^{N_p} r_\alpha \rho_\alpha U_\alpha$$

$$\Gamma = \sum_{\alpha=1}^{N_p} r_\alpha \Gamma_\alpha$$

Where r_α is the fraction, in volume, of the phase α in the control volume. This allows some simplifications to be made to the multifluid model resulting in the homogeneous model. For a given transport process, the homogeneous model assumes that the transported quantities (with the exception of volume fraction) for that process are the same for all. By the way, some displacements of the interface between the two phases (e.g. wave breaks) can result in divergence in the numerical solution.

4. RESULTS

In the next two sections Bredmose *et al.* (2003) experiments and ANSYS CFX numerical simulations are compared.

4.1. Horizontal sloshing H10

In this section, experimental and numerical results from experiment H10 of Bredmose *et al.* (2003) are compared to results obtained with ANSYS CFX. Fig. 3 shows the mesh used in the current problem. Initially, a triangular section prismatic mesh was considered, but due to convergence problems it was later replaced with a hexahedral mesh containing 18480 nodes and 9047 elements.
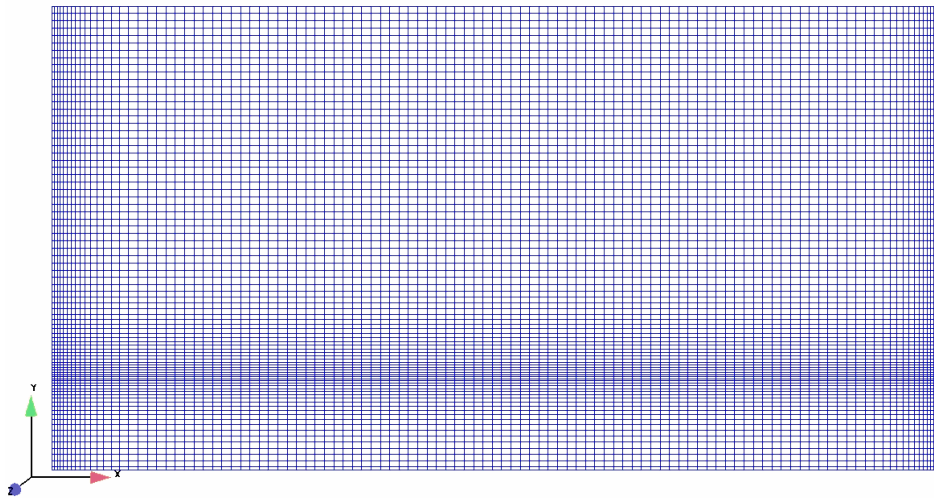
Figure 3. Hexahedral mesh used on the ANSYS CFX simulation of H10.

The no-slip boundary condition was used on both vertical walls and bottom of the container. Its top was considered to be open, while the surfaces normal to the z direction were considered symmetry planes (and the width dimension reduced for the simulation), thus making the problem two dimensional. The transient time step was set to 0.005 s, and a total simulation time of 12 s was used.

The left column in Fig. 4 shows a 12-photograph sequence taken from the H10 experiment (see Fig. 11 in Bredmose *et al.*). The dashed lines represent numerical results by the original authors using a Boussinesq model. Note that the fully nonlinear potential free surface flow solver is only used for the vertical sloshing experiments. In the right column, the corresponding results from ANSYS CFX are displayed.

The images cover the movement of the free surface immediately after the sudden change in the movement pattern observed in *t=6.21 s* (see t_2 in Fig. 1).

The sequence depicts the generated wave movement towards the left wall, followed by its impact, run-up, and subsequent reflection.

As reported by Bredmose *et al.*, the Boussinesq model fails in rough bathymetry regions, e.g. a region close to a vertical wall. Notice that the numerical results obtained with CFX are clearly more faithful to the experimental results than those calculated using the aforementioned model.

Another important feature that is missing from the Boussinesq results but present in the CFX ones is the occurrence, after the run-up, of a downward vertical jet (see Fig. 4, *t=8.04 s*).

It is good to remind that surface tension effects are not considered in the ANSYS CFX model. According to Jervis & Peregrine (1996), that can cause a 10% reduction on the maximum calculated amplitude value.
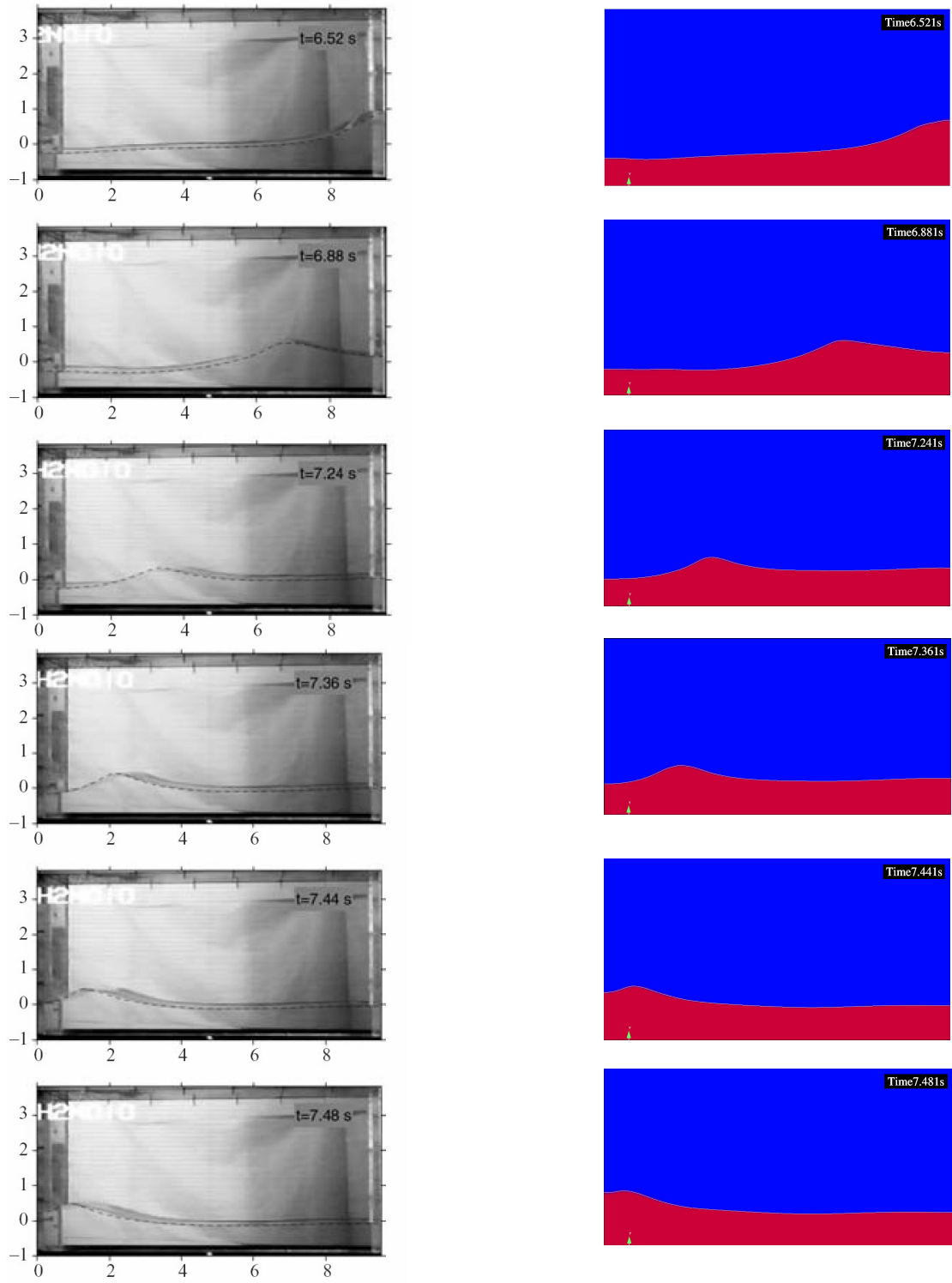
Figure 4. Comparison between experimental (H10 experiment from Bredmose *et al.* 2003) and numerical (ANSYS CFX) results.
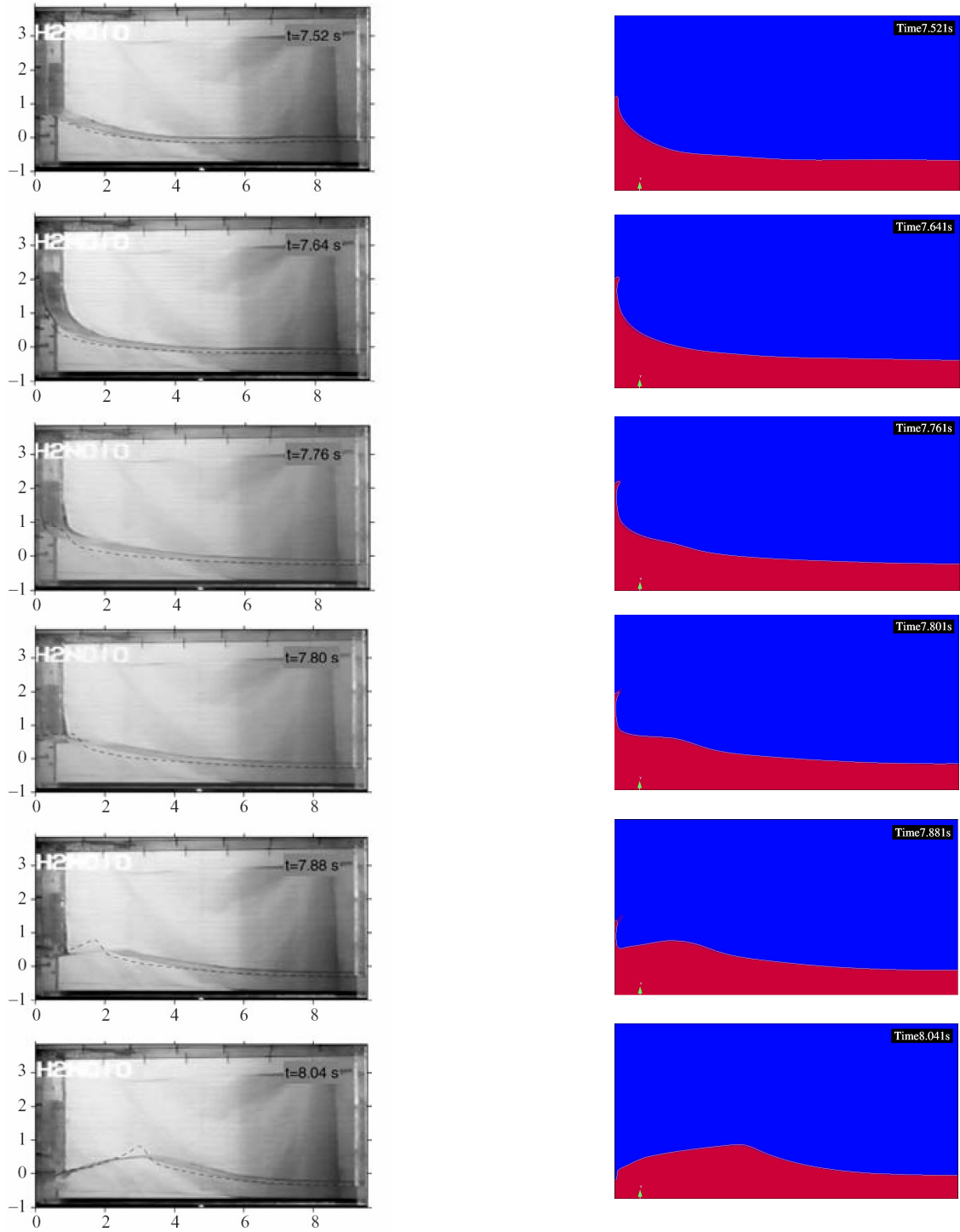
Figure 4 (cont.). Comparison between experimental (H10 experiment from Bredmose *et al.* 2003) and numerical (ANSYS CFX) results.

4.2. Vertical sloshing V21

The same boundary conditions from the H10 simulation were used. The transient time step was halved to 0.0025 seconds. This was necessary due to the displacement motion having greater frequencies, and no "smooth" starting motion being used, unlike the first section of the previous experiment displacement function (see Fig. 1).

Figure 5 depicts a similar comparison between experimental and numerical results as seen in Fig. 4, but this time with results from experiment V21. Unlike the results introduced on the previous section, the vertical sloshing simulation by ANSYS CFX does not achieve the same level of agreement with the original experimental results. This should not be understood as a complete failure, though. The numerical results were successful in predicting wave lengths; however, they failed to reproduce the non-linear features in some regions, such as wave crests and troughs, underestimating the wave amplitude.

A number of issues might have caused this outcome. Factors such as the three-dimensional nature of the phenomenon (which would prevent the emergence of good results from a two-dimensional model), poor mesh resolution, numerical dissipation caused by the finite volume method, and finally, inadequate setting of the simulation time step could all be causes for this lack of agreement. Further investigation is necessary to reach a final conclusion, and this is a probable subject for future works.

5. SUMMARY

The numerical results for the horizontal sloshing show a good agreement with Bredmose *et al.* experiments. In particular our numerical model gives a good description of the free surface's evolution when run up occurs. In fact the Boussinesq model employed by Bredmose *et al.* fails nearby the vertical wall where the free surface flow is noticeably affected by nonlinearity. For the vertical sloshing set up, more computations are necessary. Though results reproduce quite well the phase of the waves, amplitudes are underpredicted in our numerical model. This might be related to the fully nonlinear nature of the phenomena, with the appearance of Faraday waves.

6. ACKNOWLEDGEMENTS

7. REFERENCES

Billingham, J., 2002, "Nonlinear sloshing in zero gravity." *J. Fluid Mech.*, v.464, pp.365–391.

Bredmose, H., Brocchini, M., Peregrine, D.H. & Thais, L., 2003, "Experimental investigation and numerical modelling of steep forced water waves." *J. Fluid Mech.*, v.490, pp.217–249.

Dold, J.W., 1992, "An Efficient Surface-Integral Algorithm Applied to Unsteady Gravity Waves." *J. Comp. Phys.*, v.103, pp.90-115.

Dold, J.W. & Peregrine, D.H., 1986, "An efficient boundary-integral method for steep unsteady water waves." In *Numer. Meth. Fluid Dyn. II* (Eds. K.W. Morton & M.J. Baines), pp. 671–679.

Jervis, M., Peregrine, D.H., 1996, "Overtopping of waves at sea wall: a theoretical approach." *Proc. 25th Conf. Coastal ENGNG,* 2., ASCE, p.273-299.

Longuet-Higgins, M.S., 2001, "Vertical jets from standing waves: the bazooka effect." *IUTAM Symp. on Free Surface Flows*, pp. 195-203.

Mendes, A.A.O., 2007, "Geração de ondas não-lineares em um reservatório." MSc thesis, Universidade Federal Fluminense, R.J., Brazil.

Mendes, A.A.O. & Moreira, R.M., 2006, "*Sloshing* não-linear de ondas em um reservatório." *Proc. CONEM 2006*, pp.1–11.

Moreira, R.M., 2001, "Nonlinear interactions between water waves, free surface flows and singularities." PhD thesis, University of Bristol, U.K.

Ockendon, J.R. & Ockendon, H., 1973, "Resonant surface waves." *J. Fluid Mech.*, v.59, pp.397–413.

Peregrine, D.H., 2004, "Water Wave Impact on Walls." *Ann. Rev. Fluid Mech.*, v.35, pp. 1-22. 2004.

Teles da Silva, A.F., Chacaltana, J.T.A. & Moreira, R.M., 2003, "Nonlinear sloshing of gravity waves in a reservoir." *Proc. COBEM 2003*, pp.1–6.

8. RESPONSIBILITY NOTICE

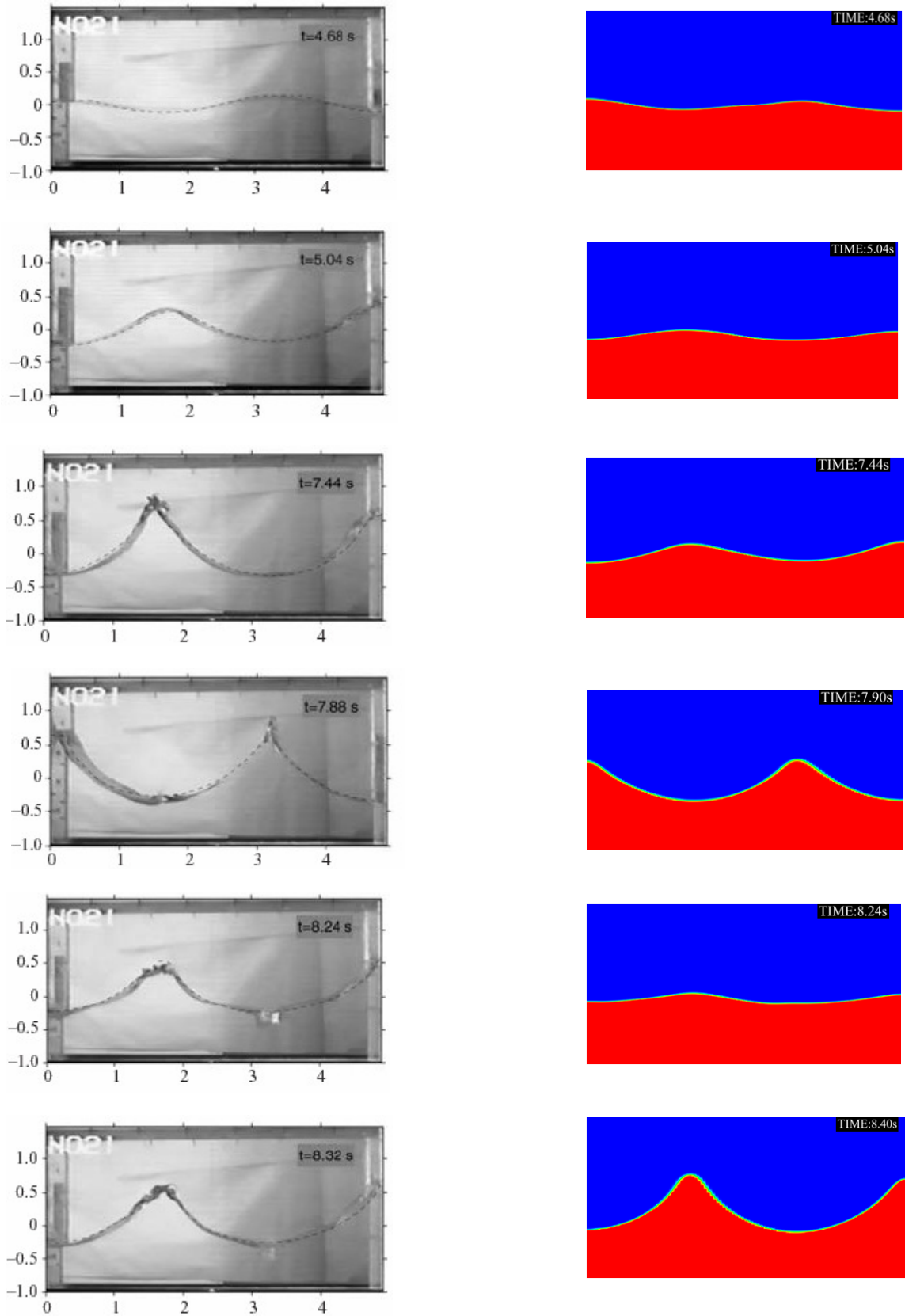The authors are the only responsible for the printed material included in this paper.

Figure 5. Comparison between experimental (V21 experiment from Bredmose *et al.* (2003)) and numerical (ANSYS CFX) results.